



Removal of aniline (Methylene Blue) and azo (Reactive Red 198) dyes by photocatalysis via nano TiO₂

Emine Basturk*, Mustafa Işık, Mustafa Karatas

Department of Environmental Engineering, Engineering Faculty, Aksaray University, 68100, Aksaray, Turkey, Tel. +90 382 288 3601; emails: eminebasturk@hotmail.com (E. Basturk), mustafaisik55@hotmail.com (M. Işık), mkaratas33@gmail.com (M. Karatas)

Received 9 June 2018; Accepted 24 November 2018

ABSTRACT

In the present study, a nano TiO₂ was used as a catalyst for the photocatalytic decolorization of Methylene Blue (MB) and Reactive Red 198 (RR198) dyes in the aqueous phase. Photocatalysis was optimized using a parametric study to improve the influence of different parameters such as catalyst dosage, pH effect, initial dye concentration, irradiation intensity for the degradation efficiency. The optimum conditions were determined as catalyst dosage= 0.25 g/L, pH = 6.5 and 9 and irradiation intensity = 50 W/m² for RR198 and MB. The color removals were 95% and 66% for RR198 and MB respectively. The efficient photocatalytic removal of selected dyes decreased with increasing initial dye concentration and increased with catalyst dosage, and also irradiation intensity. The pH effect varies the kind of dyes such as anionic and cationic. Kinetic data revealed that the decolorization was fitted by Langmuir-Hinshelwood model. The thermodynamic parameters showed that the process was feasible and exothermic. Using photocatalytic methods was a feasible choice for the removal of aniline and azo dyes.

Keywords: Methylene blue; Reactive red 198; Nano titanium dioxide; Photocatalytic decolorization

1. Introduction

Textile industries are substantial sources of environmental pollution, as they consume large amounts of water and produce enormous volume of wastewater in the dyeing and finishing operations [1]. Dyes are used as coloring substances in plethora of industries, such as various textile industry applications, food, paper, carpets, rubbers, plastics and cosmetics [2,3]. Recently it was shown that dyes and products of their degradation which could lead to the production of a great number of toxic products and in some cases even carcinogenic to humans and animals [4–6]. Therefore, it is necessary to remove these dye contaminants from wastewater before it is discharged into the environment [7]. In order to reduce the environmental impact of dyes, many technologies have been developed for the removal of dyestuffs from water and wastewater. These methods are physical,

chemical, biological, acoustic and electrical processes [8]. Several treatment approaches have been reported in literature regarding decontamination and handling of colored effluents such as membrane filtration [9], chemical treatment [10], oxidation (chlorine, hydrogen peroxide, Fenton agent) [11,12], advanced oxidation processes (AOP) [13].

Recent advances in oxidation processes draw attention to the removal of pollutants from wastewaters. These processes are economical, environmental friendly and remove dye and organic matter found in wastewater. AOPs maintain their influence in the presence of ultrasound and ultraviolet radiation [14,15]. Application of semiconductive catalysts such as iron oxide (Fe₂O₃, 2.2 eV), cadmium sulphide (CdS, 2.5 eV), ilmenite (FeTiO₃, 2.8 eV), vanadium oxide (V₂O₅, 2.8 eV), bismuth oxide (Bi₂O₃, 2.8 eV), zinc oxide (ZnO, 3.2 eV), strontium titanate (SrTiO₃, 3.4 eV), zinc sulphide (ZnS, 3.6 eV), tin oxide (SnO₂, 3.5 eV), titanium dioxide (TiO₂, 3.2 eV) [16,17]. In addition to this, novel strategy for; green synthesis of

* Corresponding author.

magnetic dummy molecularly imprinted nanoparticles, hydrophilic multi-template molecularly imprinted biopolymers, lower toxic water-compatible molecularly imprinted nanoparticles, hollow porous molecularly imprinted polymer, water-compatible (superparamagnetic) molecularly imprinted biopolymer, dummy molecularly imprinted based on functionalized silica nanoparticles were studied to bring new approach to trapping analytes [18–24].

Photocatalytic process is one of the promising approaches to enhance performance of the degradation of pollutants [1,25]. In addition to this, catalyst can be modified in order to enhance the catalytic degradation efficiency [26]. Photocatalytic process is widely used with different modified catalyst successfully for removal of different organic and azo dyes [27–32]. Among these catalysts, TiO_2 has been widely used in the catalytic processes for removing dye pollutant because of its exceptional physical, chemical and optical properties, low cost, non-toxicity, excellent catalytic activity and complete mineralization [1,33].

Herein, as explained in this work, we accumulated and combined all the advantages of materials that were mentioned above to enhance the photocatalytic efficiency of TiO_2 . Here we report the usage of TiO_2 photocatalyst homogeneously without any functionalizing the surface or using a surfactant. On the other hand, this situation brings economic advantage. From the literature, the functionalizing of the surface or using a surfactant, coating and modifying procedures are expensive.

In this study, TiO_2 nanoparticles are used for photocatalytic degradation of an azo (Reactive Red 198-RR198) and basic aniline (Methylene Blue [MB]) dye. The study has also highlighted the role of pH_{pzc} value and the different dye types (cationic and anionic) and the usage of non-modified nano TiO_2 for removal of dyes within a short time and low dosage. The influencing factors on the performance of degradation process, such as nano TiO_2 dose, initial dye concentration, pH of solution and irradiation intensity have been studied. The kinetic and thermodynamic study has been also investigated.

2. Materials and methods

2.1. Materials

TiO_2 anatase (anatase > 99%, crystalline size 10 nm) was purchased from Ege Nanotek Kimya Sanayi (Ege Nanotek Chemical Industry), Turkey. Methylene Blue ($\text{C}_{16}\text{H}_{18}\text{ClN}_3\text{S}$), NaOH, H_2SO_4 and H_2O_2 were purchased from Merck (Germany). Reactive Red 198 ($\text{C}_{27}\text{H}_{18}\text{ClN}_7\text{Na}_4\text{O}_{16}\text{S}_5$) was procured from Eksoy Kimya Sanayi ve Tic. A.Ş. (Eksoy Chemical Industry), Turkey. All the chemicals were used as received without any further purification. All solutions were prepared using ultrapure water from Milli-Q synthesis Unit (Millipore).

2.2. Catalyst characterization

X-ray diffraction (XRD) measurements of samples were carried out with X-ray diffractometer (D8 Advance X-ray Diffractometer, Bruker, USA) operating with Cu K α radiation of wavelength of 1.54059 Å at room temperature. Data were collected over 2 h values from 20 θ to 88 θ at a speed of 2 θ /min to assess the crystallinity and confirm the

structure and phase. The pH at the point of zero charge (pH_{pzc}) for catalyst was determined by the batch equilibration technique.

2.3. Analyses and experimental procedure

A stock solution of dye solution was prepared using 1 g of dye dissolved in 1 L distilled water. Dye solution of known concentration were prepared in distilled water, mixed appropriate amount of TiO_2 and dispersed in the photoreactor. The pH of the dye solution was adjusted either using H_2SO_4 or NaOH. The experimental procedure has been given in details in our previous papers [34,35]. UV–Vis spectrophotometer (UV 1280, Shimadzu, Japan) was used to monitor the dye degradation or removal process. Typically, during the course of reaction, 1 mL of dye samples was withdrawn using a micro pipette, centrifuged and filtered to ensure catalyst color removal from the dye solution. Maximum dye absorbance wavelength (λ_{max}) was used for absorbance measurement. The calibration equation of RR198 and MB are $y = 0.0194x - 0.0032$ and $y = 0.0248 + 0.0046x$, respectively ($y = \text{absorbance}$ and $x = \text{dye concentration}$). The characteristics of selected dyes are shown in Table 1.

3. Results and discussion

3.1. Characterization and catalytic effect of catalyst

The crystal structure of the catalyst was identified by X-ray diffractometer. The pH at the point of zero charge (pH_{pzc}) for catalyst was determined by the batch equilibration technique. The XRD and pH_{pzc} results are shown in Figs. 1 and 2.

According to the XRD results, the maximum peak value $2\theta = 25.3$. In addition, the high peak values show that the material used TiO_2 is anatase type as same in literature (Fig. 1) [36]. The pH_{pzc} was found to be 7.41 (Fig. 2).

Table 1
Characteristics of selected dyes

	Methylene Blue	Reactive Red 198
CAS No	122965-43-9	145017-98-7
Dye type	Basic aniline	Azo
Molecular weight	319.86	984.183
Molecular formula	$\text{C}_{16}\text{H}_{18}\text{ClN}_3\text{S}$	$\text{C}_{27}\text{H}_{18}\text{ClN}_7\text{Na}_4\text{O}_{16}\text{S}_5$
λ_{max}	664	520

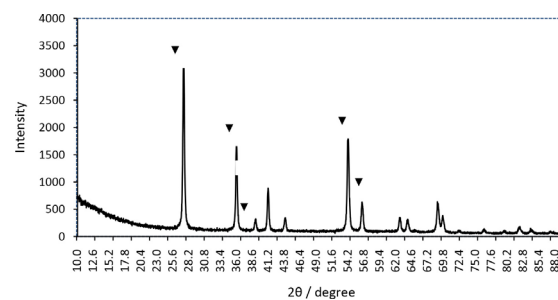


Fig. 1. XRD graph of nano TiO_2 (▼: anatase type).

3.2. Effect of catalyst dosage

Fig. 3 shows the effect of catalyst dosage on the photocatalytic decolorization of RR198 and MB. As shown, at catalyst dosages of 0.05, 0.1 and 0.25 g/L, the catalytic decolorization of RR198 and MB were found to be 95% and 56%. The optimum catalyst dosage was chosen as 0.25 g/L (Fig. 3). The increasing the catalyst dosage provides more active areas which leads to dye removal [37]. Furthermore, with the increase of the number of photons which occurred by UV radiation and absorbed by the TiO_2 particles, more electrons are generated from the valence band to the transmission band. The result of increasing the amount of catalyst, the number of active areas (hydroxyl and superoxide ion) in the surface is increasing [38–40]. Above the optimum dosage, the UV penetration is reduced [41].

Another factor that may be responsible for the lower degradation is agglomeration of particles at high concentrations (despite the effect of ultrasound to disaggregate) that leads to increase in the specific surface area [41–44]. Furthermore, the attraction of the particles towards each other can deactivate the active particles which reduce the removal efficiency of the target dyes [45]. Using high amount of nano- TiO_2 particles, there is not any molecules react for adsorption. There are two reasons for this: (i) excess catalyst will diminish the hydroxyl radical and reduce the removal efficiency by blocking the UV radiation [46] and (ii) light scattering increases and UV penetration decreases [44]. The equation for the overloading of TiO_2 is shown below:



where TiO_2^* is the active species which is adsorbed onto the surface and $\text{TiO}_2^\#$ is the deactivated form of TiO_2 . Result of overloading of catalyst is the precipitation of TiO_2 [47]. Therefore, the use of TiO_2 at high doses is not very useful due to these effects.

3.3. pH effect

pH is an important operating parameter in the heterogeneous photocatalysis, since it determines the surface charge properties of the photocatalyst and therefore the adsorption behavior of the pollutant and also the size of aggregate it forms [39]. The surface charge of TiO_2 is the function of pH value of aqueous solution. When a nanoparticle is dispersed in an aqueous solution, the surface ionization results in production of the surface charge. The ionization on catalyst surface which is the protonation and deprotonation under the acidic and alkaline conditions is shown in Eqs. (2) and (3) as follows:



The catalyst surface charge is dependent on the pH of aqueous solution. As noted in literature, the pH_{pzc} value is used at pH studies [48,49]. When $\text{pH} < \text{pH}_{\text{pzc}}$, the catalyst surface is charged positive and the electrostatic attraction may occur between the negatively charged pollutants and catalyst. These attractions increase the adsorption of photons which occur as a result of photocatalytic reactions [39]. Conversely, due to the coulombic repulsion, anionic pollutants [50] cannot be adsorbed but cationic pollutants can be easily adsorbed on catalyst surface [51]. Because of this, the RR198 dye removal is high at acidic conditions and vice versa for MB (Figs. 4 and 5).

3.4. Effect of irradiation intensity

Experiments were performed to study the variations in the rate of degradation at different irradiation intensity. The degradation increases with increase in UV intensity as

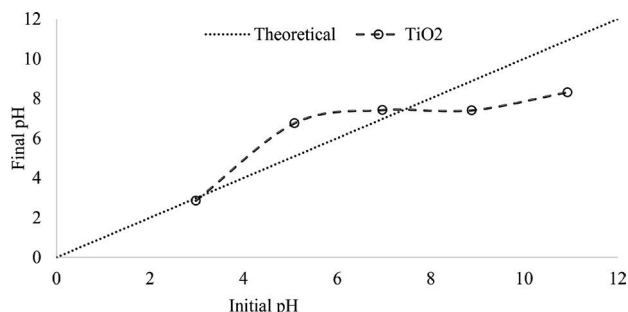


Fig. 2. pH_{pzc} graph of nano TiO_2 (catalyst dosage = 0.25 g/L).

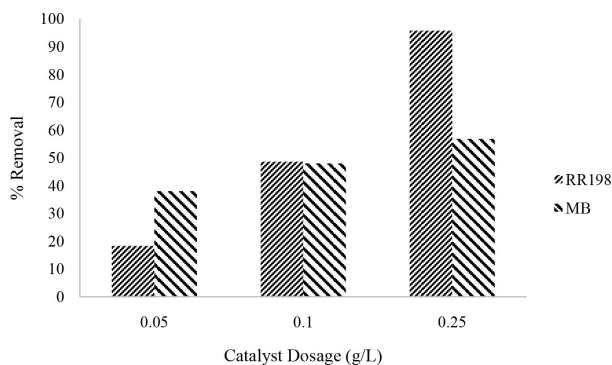


Fig. 3. Effect of catalyst dosage for selected dyes ([RR198] = 100 mg/L, pH = 6.55 (MB), pH = 6.55 (RR198), UV light intensity = 50 W/m^2 , time = 15 min).

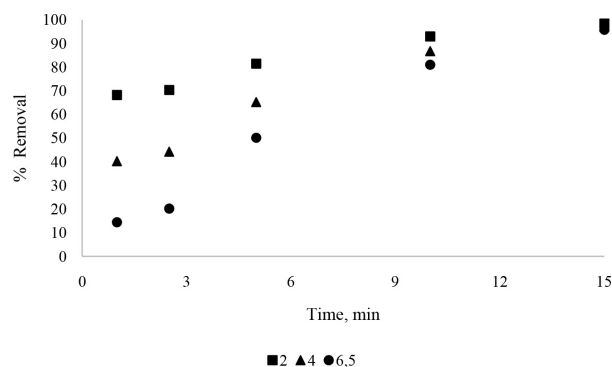


Fig. 4. pH effect of RR198 removal ([RR198]=100 mg/L, catalyst dosage= 0.25 g/L, UV light intensity= 50 W/m^2).

more radiations occur on the nano-TiO₂. As a result, more OH radicals are produced which proceed to high removal of selected dyes [52]. As can be seen in Fig. 6, there is a similar relationship between light intensity and dye removal.

3.5. Effect of initial concentration of dye

Fig. 7 displays the effect of various initial dye concentrations on removal efficiency. Increase in the dye concentration from 25 to 100 mg/L decreases the percentage removal of RR198 from 53% to 37% and also MB from 71% to 50% in 5 min of irradiation time (Fig. 7). The clogging of active sites on the nanocomposite surface makes the sorption become less

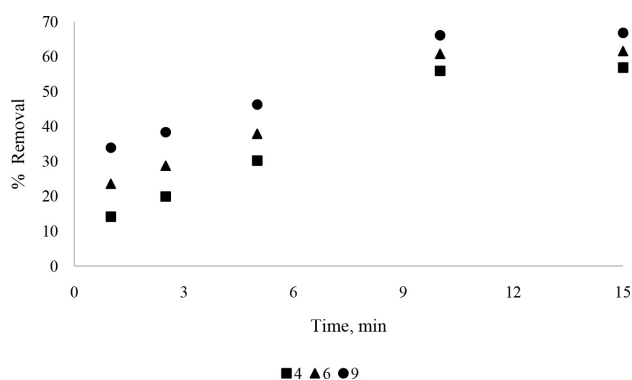


Fig. 5. pH effect of MB removal ([MB]=100 mg/L, catalyst dosage = 0.25 g/L, UV light intensity = 50 W/m²).

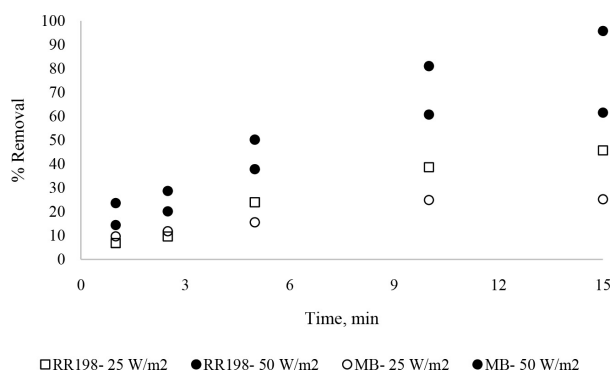


Fig. 6. Irradiation intensity effect ([MB-RR198] = 100 mg/L, catalyst dosage = 0.25 g/L, pH = 9 [MB], pH = 6.5 [RR198]).

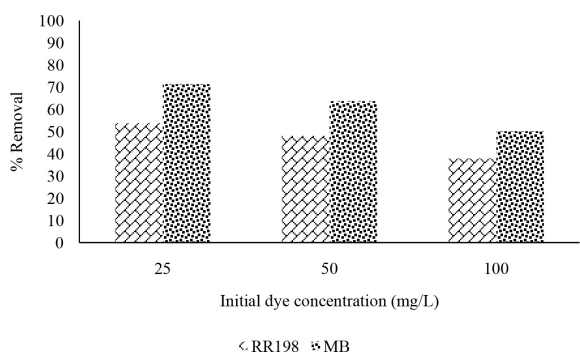


Fig. 7. Initial dye concentration effect (catalyst dosage = 0.25 g/L, pH = 9 (MB), pH = 6 (RR198), UV light intensity = 50 W/m²).

efficient; furthermore, decolorization efficiency is inversely affected by dye concentration [53]. This is due to decrease in the path length of photon entering into the dye solution and a more impermeable solution to incident light, which leads to a lower efficiency of light utilization at high dye concentration [54,55]. In addition to this, the hydroxyl radicals formed on the surface of TiO₂ decreases, the relative number of radicals attacking the dye decreases and thus removal efficiency decreases [52]. Our observations are in agreement with that reported by previous studies [53,54,56]. It was also concluded from Table 2 that dye removal by UV/TiO₂ photocatalytic oxidation was an efficient method by the comparison of similar studies in the literature.

3.6. Kinetic study

Heterogeneous photocatalytic dye degradation reactions at solid-liquid interface are generally well fitted with Langmuir-Hinshelwood rate expression [64]. The kinetic studies on photocatalytic decolorization of selected dyes in the presence of TiO₂ catalyst were investigated according to the Langmuir-Hinshelwood kinetic model which is indicated in previous works in the literature [56,64–70]. The rate of degradation can be described by a pseudo-first-order Langmuir-Hinshelwood kinetic model (Eq. (4)) [71]:

$$r = -\frac{dC}{dt} = \frac{CKkr}{1 + KC} \quad (4)$$

where r stands for the rate of degradation, K represents the equilibrium constant for the adsorption of selected dyes on the catalyst surface, and kr corresponds to the reaction constant. This equation can also be written in the following form:

$$\frac{\ln C_0}{C} \approx krKt = k't \quad (5)$$

The kinetic model was applied by plotting $\ln(C_0/C)$ vs. t , where C_0 is the initial concentration of dye, and C is the concentration of dye at time t . It was clearly shown in Fig. 8, a linear relationship follows the $\ln(C/C_0)$ vs. time. The slope corresponds to the apparent first-order rate constant (k , min⁻¹). The pseudo-first-order rate constant, k , was evaluated from the slope of the $\ln(C_0/C)$ vs. time plots. All regression coefficients R^2 greater than 0.88, indicated that the experimental results followed first-order kinetic model. The obtained constant rates of removal at photocatalysis are shown in Table 3

3.7. Thermodynamic study

Three thermodynamic parameters, free energy change (ΔG^0), enthalpy change (ΔH^0) and entropy change (ΔS^0) were prescribed by the resulting equations [35,53,72]:

$$\Delta G = -RT \ln k \quad (6)$$

$$\ln k = \ln A - \left(\frac{E_a}{RT} \right) \quad (7)$$

Table 2
Photocatalytic dye removal efficiencies with various nanocatalysts (%)

Dye	Catalyst	Catalyst amount/ concentration	pH	Removal efficiency (%)	Time (min)	Sources
Methyl Orange (3×10^{-5} M)	TiO ₂ nanobelt	200 mg	4	≈90	60	[57]
Methylene Blue (5×10^{-5} M)	ZnO/NiFe ₂ O ₄ nanoparticles	1.5 g/L	–	≈92	70	[58]
Rhodamine B, Methylene Blue and Texbrite (20 mg/L)	Graphene-Bi ₃ La ₁₀ O ₂₇ -zeolite nanocomposite	1 g/L	7	85, 87, 83	5	[59]
Methylene Blue, Methyl Orange	TiO ₂ -GO nanocomposite	0.4 g/L	Neutral	100, 84	25, 240	[60]
Malachite Green (100 mg/L)	Au/NaNbO ₃ nanoparticles	3.6 g/L	–	94	60	[61]
Congo Red, Bismarck Brown (0.2 mM)	Ag/rGO nanocomposite	1 g/L	3, 11	≈94, ≈99	120	[62]
Remazol Brilliant Red X-3BS, Rhodamine-B (10 mg/L)	Sb ₂ S ₃ /rGO	0.2 g/L	–	≈93, ≈90	150	[27]
Congo Red (75 mg/L)	ZnO/ZnSe	0.4 g/L	–	91	40	[28]
Rhodamine B, Methylene Blue, Methyl Orange	ZnFe ₂ O ₄ /G and ZnFe ₂ O ₄ /G-H ₂ O ₂	0.5 g/L	5, 6, 5	≈100	120	[63]
Rhodamine B, Mixed dye wastewater (Methyl Orange, Orange IV and Malachite Green) (25,10 mg/L)	Sn-doped BiOCl	0.5 g/L	6	≈99	480	[29]
Rhodamine B	CeO ₂ /Y ₂ O ₃	0.4 g/L	7	≈ 96	180	[31]
Methyl Red (1×10^{-5} M)	NiO/PdO	3 g/L	4	≈ 99	90	[30]
Methyl orange, Rhodamine B (50 mg/L)	BiFeO ₃ /CuWO ₄	0.1 g/L	–	≈ 87, ≈ 85	120, 75	[32]
Reactive Red 198, Methylene Blue (100 mg/L)	Nano TiO ₂ -10 nm	0.25 g/L	2, 9	≈ 95, ≈ 66	15	This study

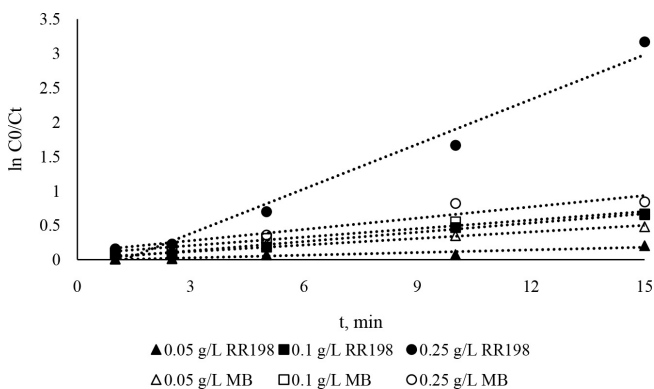


Fig. 8. Plot of $\ln C_0/C$ vs. time t on decolorization of selected dyes ([MB-RR198] = 100 mg/L, pH = 9 (MB), pH = 6.5 (RR198), time = 15 min).

$$\ln k = \left(\Delta \frac{S}{R} \right) - \left(\Delta \frac{H}{RT} \right) \quad (8)$$

where R is the universal gas constant, $8.314 \text{ J mol}^{-1} \text{ K}^{-1}$; T is the absolute temperature (K), and k is the Langmuir constant (mol L^{-1}). ΔS^0 and ΔH^0 could be obtained from the slope and intercept $\ln k$ vs. $1/T$ according to Eq. (8). Values of ΔS^0 , ΔH^0 and ΔG^0 are presented in Table 4. Results show that ΔH^0 values (Tables 4) are negative. So the process was exothermic.

Table 3
Value of kinetic constants for photocatalytic system ([MB-RR198] = 100 mg/L, catalyst dosage = 0.25 g/L, pH = 9 (MB), pH = 6, 5 (RR198), time = 15 min)

Catalyst dosage	RR198		MB	
	k	R^2	k	R^2
0.05 g/L	0.0127	0.8848	0.0317	0.9644
0.1 g/L	0.0449	0.9814	0.0412	0.9670
0.25 g/L	0.2167	0.9764	0.0546	0.9172

The negative values of ΔS^0 relate to a lessening in degree of freedom of the adsorbed species. The positive value for the Gibbs free energy showed that the process was not spontaneous in nature. According to the results, we cannot say certain expressions, also, the reaction pathway involved in the dye degradation is complex, with many unknown reactions occurring.

4. Conclusions

The removal of aniline and azo dyes on nano TiO₂ is an effective method of enhancing the photocatalytic activity of the semiconductor as demonstrated in this study. Materials with more surface area provide better performance as they will create more area for photocatalytic reactions. The enhancement was related to the size of the particles and the

Table 4

Thermodynamic parameters for the decolorization of RR198 and MB by photo oxidation ([MB-RR198] = 100 mg/L, catalyst dosage = 0.25 g/L, pH = 9 (MB), pH = 6.5 (RR198), time = 15 min)

T (K)	MB			RR198		
	ΔS^0 (kJ/mol K)	$\Delta H^0 - Ea$ (kJ/mol)	ΔG^0 (kJ/mol)	ΔS^0 (kJ/mol K)	$\Delta H^0 - Ea$ (kJ/mol)	ΔG^0 (kJ/mol)
273	-0.0132	-0.357	4.249	-0.0010	-6.578	6.302
293			4.383			6.211
303			4.514			6.285

surface properties that allowed more efficient adsorption and oxygenated species. We report the usage of TiO₂ photocatalyst homogeneously that brings economic advantage, without any functionalizing of the surface or using a surfactant. From the literature, functionalizing the surface or using a surfactant, coating and modifying procedures are expensive and at the same time the higher removal efficiency was obtained without any modifications. Different performance of the catalysts under UV irradiation was attributed to different operational conditions. The optimum conditions were determined as catalyst dosage = 0.25 g/L, pH = 6.5 and 9 and irradiation intensity = 50 W/m² for RR198 and MB. The color removals were 95% and 66% for RR198 and MB, respectively. The study has also highlighted the role of pH_{pzc} value and the different dye types (cationic and anionic). As compared with other studies, however, usage of nano TiO₂ has some disadvantages such as recovery. In our next study, as a solution to this problem, we will work to fix the TiO₂ material to the films, the porous support materials or the membranes. The present work has clearly demonstrated the efficacy of these treatment approaches for removal of basic aniline and azo dyes.

Acknowledgment

This work was supported by Aksaray University Scientific Research Projects Coordinatorship (2016-046 project).

References

- [1] A. Khataee, M. Sheydaei, A. Hassani, M. Taseidifar, S. Karaca, Sonocatalytic removal of an organic dye using TiO₂/montmorillonite nanocomposite, *Ultrason. Sonochem.*, 22 (2015) 404–411.
- [2] M. Muruganandham, R. Amutha, G.-J. Lee, S.-H. Hsieh, J.J. Wu, M. Sillanpää, Facile fabrication of tunable Bi₂O₃ self-assembly and its visible light photocatalytic activity, *J. Phys. Chem. C*, 116 (2012) 12906–12915.
- [3] S. Jafari, F. Zhao, D. Zhao, M. Lahtinen, A. Bhatnagar, M. Sillanpää, A comparative study for the removal of methylene blue dye by N and S modified TiO₂ adsorbents, *J. Mol. Liq.*, 207 (2015) 90–98.
- [4] A. Sandoval, C. Hernández-Ventura, T.E. Klimova, Titanate nanotubes for removal of methylene blue dye by combined adsorption and photocatalysis, *Fuel*, 198 (2017) 22–30.
- [5] M. Rafatullah, O. Sulaiman, R. Hashim, A. Ahmad, Adsorption of methylene blue on low-cost adsorbents: a review, *J. Hazard. Mater.*, 177 (2010) 70–80.
- [6] Z.-D. Meng, W.-C. Oh, Sonocatalytic degradation and catalytic activities for MB solution of Fe treated fullerene/TiO₂ composite with different ultrasonic intensity, *Ultrason. Sonochem.*, 18 (2011) 757–764.
- [7] P. Nuengmatcha, S. Chanthai, R. Mahachai, W.-C. Oh, Sonocatalytic performance of ZnO/graphene/TiO₂ nanocomposite for degradation of dye pollutants (methylene blue, texbrite BAC-L, texbrite BBU-L and texbrite NFW-L) under ultrasonic irradiation, *Dyes Pigm.*, 134 (2016) 487–497.
- [8] V. Gupta, Application of low-cost adsorbents for dye removal—a review, *J. Environ. Manage.*, 90 (2009) 2313–2342.
- [9] S. Avlonitis, I. Poullos, D. Sotiriou, M. Pappas, K. Moutesidis, Simulated cotton dye effluents treatment and reuse by nanofiltration, *Desalination*, 221 (2008) 259–267.
- [10] Y. Zhou, Z. Liang, Y. Wang, Decolorization and COD removal of secondary yeast wastewater effluents by coagulation using aluminum sulfate, *Desalination*, 225 (2008) 301–311.
- [11] S. Wang, A comparative study of Fenton and Fenton-like reaction kinetics in decolourisation of wastewater, *Dyes Pigm.*, 76 (2008) 714–720.
- [12] R. Hage, A. Lienke, Applications of transition - metal catalysts to textile and wood - pulp bleaching, *Angew. Chem., Int. Ed.*, 45 (2006) 206–222.
- [13] A. Khataee, R.D.C. Soltani, A. Karimi, S.W. Joo, Sonocatalytic degradation of a textile dye over Gd-doped ZnO nanoparticles synthesized through sonochemical process, *Ultrason. Sonochem.*, 23 (2015) 219–230.
- [14] P. Srivastava, S. Goyal, R. Tayade, Ultrasound-assisted adsorption of reactive blue 21 dye on TiO₂ in the presence of some rare earths (La, Ce, Pr and Gd), *Canad. J. Chem. Eng.*, 92 (2014) 41–51.
- [15] A. Aleboeyeh, M.B. Kasiri, H. Aleboeyeh, Influence of dyeing auxiliaries on AB74 dye degradation by UV/H₂O₂ process, *J. Environ. Manage.*, 113 (2012) 426–431.
- [16] H. Huang, D.Y. Leung, P.C. Kwong, J. Xiong, L. Zhang, Enhanced photocatalytic degradation of methylene blue under vacuum ultraviolet irradiation, *Catal. Today*, 201 (2013) 189–194.
- [17] T.S. Natarajan, K. Natarajan, H.C. Bajaj, R.J. Tayade, Enhanced photocatalytic activity of bismuth-doped TiO₂ nanotubes under direct sunlight irradiation for degradation of Rhodamine B dye, *J. Nanopart. Res.*, 15 (2013) 1669.
- [18] M. Arabi, A. Ostovan, M. Ghaedi, M.K. Purkait, Novel strategy for synthesis of magnetic dummy molecularly imprinted nanoparticles based on functionalized silica as an efficient sorbent for the determination of acrylamide in potato chips: optimization by experimental design methodology, *Talanta*, 154 (2016) 526–532.
- [19] A. Ostovan, M. Ghaedi, M. Arabi, Q. Yang, J. Li, L. Chen, Hydrophilic multitemplate molecularly imprinted biopolymers based on a green synthesis strategy for determination of B-family vitamins, *ACS Appl. Mater. Interface*, 10 (2018) 4140–4150.
- [20] M. Arabi, M. Ghaedi, A. Ostovan, Development of a lower toxic approach based on green synthesis of water-compatible molecularly imprinted nanoparticles for the extraction of hydrochlorothiazide from human urine, *ACS Sustain. Chem. Eng.*, 5 (2017) 3775–3785.
- [21] A. Ostovan, M. Ghaedi, M. Arabi, A. Asfaram, Hollow porous molecularly imprinted polymer for highly selective clean-up followed by influential preconcentration of ultra-trace glibenclamide from bio-fluid, *J. Chromatogr. A*, 1520 (2017) 65–74.
- [22] A. Ostovan, M. Ghaedi, M. Arabi, Fabrication of water-compatible superparamagnetic molecularly imprinted biopolymer for clean separation of baclofen from bio-fluid samples: a mild and green approach, *Talanta*, 179 (2018) 760–768.

- [23] M. Arabi, M. Ghaedi, A. Ostovan, Water compatible molecularly imprinted nanoparticles as a restricted access material for extraction of hippuric acid, a biological indicator of toluene exposure, from human urine, *Microchim. Acta*, 184 (2017) 879–887.
- [24] M. Arabi, M. Ghaedi, A. Ostovan, Development of dummy molecularly imprinted based on functionalized silica nanoparticles for determination of acrylamide in processed food by matrix solid phase dispersion, *Food Chem.*, 210 (2016) 78–84.
- [25] J. Wang, Z. Jiang, Z. Zhang, Y. Xie, Y. Lv, J. Li, Y. Deng, X. Zhang, Study on inorganic oxidants assisted sonocatalytic degradation of Acid Red B in presence of nano-sized ZnO powder, *Sep. Purif. Technol.*, 67 (2009) 38–43.
- [26] T.S. Natarajan, H.C. Bajaj, R.J. Tayade, Synthesis of homogeneous sphere-like Bi_2WO_6 nanostructure by silica protected calcination with high visible-light-driven photocatalytic activity under direct sunlight, *Cryst. Eng. Comm.*, 17 (2015) 1037–1049.
- [27] L. Dashairya, M. Sharma, S. Basu, P. Saha, Enhanced dye degradation using hydrothermally synthesized nanostructured $\text{Sb}_2\text{S}_3/\text{rGO}$ under visible light irradiation, *J. Alloys Comp.*, 735 (2018) 234–245.
- [28] M.F. Ehsan, S. Bashir, S. Hamid, A. Zia, Y. Abbas, K. Umbreen, M.N. Ashiq, A. Shah, One-pot facile synthesis of the ZnO/ZnSe heterostructures for efficient photocatalytic degradation of azo dye, *Appl. Surf. Sci.*, 459 (2018) 194–200.
- [29] X. Han, S. Dong, C. Yu, Y. Wang, K. Yang, J. Sun, Controllable synthesis of Sn-doped BiOCl for efficient photocatalytic degradation of mixed-dye wastewater under natural sunlight irradiation, *J. Alloys Comp.*, 685 (2016) 997–1007.
- [30] O. Omotunde, A. Okoronkwo, A. Aiyesanmi, E. Gurgur, Photocatalytic behavior of mixed oxide NiO/PdO nanoparticles toward degradation of methyl red in water, *J. Photochem. Photobiol., A*, 365 (2018) 145–150.
- [31] C.M. Magdalane, K. Kaviyarasu, J.J. Vijaya, B. Siddhardha, B. Jeyaraj, J. Kennedy, M. Maaza, Evaluation on the heterostructured $\text{CeO}_2/\text{Y}_2\text{O}_3$ binary metal oxide nanocomposites for UV/Vis light induced photocatalytic degradation of Rhodamine-B dye for textile engineering application, *J. Alloys Comp.*, 727 (2017) 1324–1337.
- [32] H. Ramezanalizadeh, F. Manteghi, Design and development of a novel $\text{BiFeO}_3/\text{CuWO}_4$ heterojunction with enhanced photocatalytic performance for the degradation of organic dyes, *J. Photochem. Photobiol., A*, 338 (2017) 60–71.
- [33] L. Zhu, Z.-D. Meng, C.-Y. Park, T. Ghosh, W.-C. Oh, Characterization and relative sonocatalytic efficiencies of a new MWCNT and CdS modified TiO_2 catalysts and their application in the sonocatalytic degradation of rhodamine B, *Ultrason. Sonochem.*, 20 (2013) 478–484.
- [34] E. Basturk, M. Karatas, Advanced oxidation of reactive blue 181 solution: a comparison between fenton and sono-fenton process, *Ultrason. Sonochem.*, 21 (2014) 1881–1885.
- [35] E. Basturk, M. Karatas, Decolorization of anthraquinone dye Reactive Blue 181 solution by UV/ H_2O_2 process, *J. Photochem. Photobiol., A*, 299 (2015) 67–72.
- [36] G. Liao, D. Zhu, J. Zheng, J. Yin, B. Lan, L. Li, Efficient mineralization of bisphenol A by photocatalytic ozonation with TiO_2 -graphene hybrid, *J. Taiwan Inst. Chem. Eng.*, 67 (2016) 300–305.
- [37] K. Byrappa, A. Subramani, S. Ananda, K.L. Rai, R. Dinesh, M. Yoshimura, Photocatalytic degradation of rhodamine B dye using hydrothermally synthesized ZnO, *Bull. Mater. Sci.*, 29 (2006) 433–438.
- [38] W.A. Sadik, A.W. Nashed, A.-G.M. El-Demerdash, Photodecolourization of ponceau 4R by heterogeneous photocatalysis, *J. Photochem. Photobiol., A*, 189 (2007) 135–140.
- [39] H. Hamad, W. Sadik, M.A. El-Latif, A. Kashyout, M. Feteha, Photocatalytic parameters and kinetic study for degradation of dichlorophenol-indophenol (DCPIP) dye using highly active mesoporous TiO_2 nanoparticles, *J. Environ. Sci.*, 43 (2016) 26–39.
- [40] S. Zhu, X. Yang, W. Yang, L. Zhang, J. Wang, M. Huo, Application of porous nickel-coated TiO_2 for the photocatalytic degradation of aqueous quinoline in an internal airlift loop reactor, *Int. J. Environ. Res. Public Health*, 9 (2012) 548–563.
- [41] A. Ziyilan-Yavas, Y. Mizukoshi, Y. Maeda, N.H. Ince, Supporting of pristine TiO_2 with noble metals to enhance the oxidation and mineralization of paracetamol by sonolysis and sonophotolysis, *Appl. Catal., B*, 172 (2015) 7–17.
- [42] S. Kavitha, P. Palanisamy, Photocatalytic and sonophotocatalytic degradation of reactive red 120 using dye sensitized TiO_2 under visible light, *Int. J. Civil Environ. Eng.*, 3 (2011) 1–6.
- [43] A. Ajmal, I. Majeed, R. Malik, M. Iqbal, M.A. Nadeem, I. Hussain, S. Yousaf, G. Mustafa, M. Zafar, M.A. Nadeem, Photocatalytic degradation of textile dyes on $\text{Cu}_2\text{O-CuO/TiO}_2$ anatase powders, *J. Environ. Chem. Eng.*, 4 (2016) 2138–2146.
- [44] N.F. Zainudin, A.Z. Abdullah, A.R. Mohamed, Characteristics of supported nano- $\text{TiO}_2/\text{ZSM-5/silica}$ gel (SNTZS): photocatalytic degradation of phenol, *J. Hazard. Mater.*, 174 (2010) 299–306.
- [45] B. Neppolian, H. Choi, S. Sakthivel, B. Arabindoo, V. Murugesan, Solar light induced and TiO_2 assisted degradation of textile dye reactive blue 4, *Chemosphere*, 46 (2002) 1173–1181.
- [46] U. Akpan, B. Hameed, Parameters affecting the photocatalytic degradation of dyes using TiO_2 -based photocatalysts: a review, *J. Hazard. Mater.*, 170 (2009) 520–529.
- [47] N. San, M. Kılıç, Z. Tuiebakhova, Z. Çınar, Enhancement and modeling of the photocatalytic degradation of benzoic acid, *J. Adv. Oxid. Technol.*, 10 (2007) 43–50.
- [48] M.N. Chong, B. Jin, H. Zhu, C. Chow, C. Saint, Application of H-titanate nanofibers for degradation of Congo Red in an annular slurry photoreactor, *Chem. Eng. J.*, 150 (2009) 49–54.
- [49] I.J. Ochuma, R.P. Fishwick, J. Wood, J.M. Winterbottom, Optimisation of degradation conditions of 1, 8-diazabicyclo [5.4. 0] undec-7-ene in water and reaction kinetics analysis using a cocurrent downflow contactor photocatalytic reactor, *Appl. Catal., B*, 73 (2007) 259–268.
- [50] M.L. Škorić, I. Terzić, N. Milosavljević, M. Radetić, Z. Šaponjić, M. Radoičić, M.K. Krušić, Chitosan-based microparticles for immobilization of TiO_2 nanoparticles and their application for photodegradation of textile dyes, *Eur. Polym. J.*, 82 (2016) 57–70.
- [51] W. Chu, W. Choy, T. So, The effect of solution pH and peroxide in the TiO_2 -induced photocatalysis of chlorinated aniline, *J. Hazard. Mater.*, 141 (2007) 86–91.
- [52] A.P. Toor, A. Verma, C. Jotshi, P. Bajpai, V. Singh, Photocatalytic degradation of Direct Yellow 12 dye using UV/ TiO_2 in a shallow pond slurry reactor, *Dyes Pigm.*, 68 (2006) 53–60.
- [53] Z.H. Siahpoosh, M. Soleimani, Photocatalytic degradation of azo anionic dye (RR120) in ZnO-Ghezaljel nanoclay composite catalyst/UV-C system: equilibrium, kinetic and thermodynamic studies, *Process Saf. Environ. Protect.*, 111 (2017) 180–193.
- [54] L. Hu, G. Deng, W. Lu, S. Pang, X. Hu, Deposition of CdS nanoparticles on MIL-53 (Fe) metal-organic framework with enhanced photocatalytic degradation of RhB under visible light irradiation, *Appl. Surf. Sci.*, 410 (2017) 401–413.
- [55] M. Muruganandham, N. Sobana, M. Swaminathan, Solar assisted photocatalytic and photochemical degradation of Reactive Black 5, *J. Hazard. Mater.*, 137 (2006) 1371–1376.
- [56] N. Chekir, D. Tassalit, O. Benhabiles, N.K. Merzouk, M. Ghenna, A. Abdessemed, R. Issaadi, A comparative study of tartrazine degradation using UV and solar fixed bed reactors, *Int. J. Hydrogen Energy*, 42 (2017) 8948–8954.
- [57] D.P. Kumar, N.L. Reddy, M. Karthikeyan, N. Chinniah, V. Bramhaiah, V.D. Kumari, M. Shankar, Synergistic effect of nanocavities in anatase TiO_2 nanobelts for photocatalytic degradation of methyl orange dye in aqueous solution, *J. Colloid Interface Sci.*, 477 (2016) 201–208.
- [58] J. Adeleke, T. Theivasanthi, M. Thiruppathi, M. Swaminathan, T. Akomolafe, A. Alabi, Photocatalytic degradation of methylene blue by $\text{ZnO/NiFe}_2\text{O}_4$ nanoparticles, *Appl. Surf. Sci.*, 455 (2018) 195–200.
- [59] Y. Areerob, K.-Y. Cho, W.-C. Oh, Microwave assisted synthesis of graphene- $\text{Bi}_5\text{La}_{10}\text{O}_{27}$ -zeolite nanocomposite with efficient photocatalytic activity towards organic dye degradation, *J. Photochem. Photobiol., A*, 340 (2017) 157–169.
- [60] R. Atchudan, T.N.J.I. Edison, S. Perumal, D. Karthikeyan, Y.R. Lee, Effective photocatalytic degradation of anthropogenic dyes

- using graphene oxide grafting titanium dioxide nanoparticles under UV-light irradiation, *J. Photochem. Photobiol., A*, 333 (2017) 92–104.
- [61] E. Baeissa, Photocatalytic degradation of malachite green dye using Au/NaNbO₃ nanoparticles, *J. Alloys Comp.*, 672 (2016) 564–570.
- [62] P. Borthakur, P.K. Boruah, N. Hussain, Y. Silla, M.R. Das, Specific ion effect on the surface properties of Ag/reduced graphene oxide nanocomposite and its influence on photocatalytic efficiency towards azo dye degradation, *Appl. Surf. Sci.*, 423 (2017) 752–761.
- [63] D. Lu, Y. Zhang, S. Lin, L. Wang, C. Wang, Synthesis of magnetic ZnFe₂O₄/graphene composite and its application in photocatalytic degradation of dyes, *J. Alloys Comp.*, 579 (2013) 336–342.
- [64] Ö. Kerkez-Kuyumcu, E. Kibar, K. Dayıoğlu, F. Gedik, A.N. Akın, Ş. Özkara-Aydınoglu, A comparative study for removal of different dyes over M/TiO₂ (M = Cu, Ni, Co, Fe, Mn and Cr) photocatalysts under visible light irradiation, *J. Photochem. Photobiol., A*, 311 (2015) 176–185.
- [65] R. Pol, M. Guerrero, E. García-Lecina, A. Altube, E. Rossinyol, S. Garroni, M.D. Baró, J. Pons, J. Sort, E. Pellicer, Ni-, Pt- and (Ni/Pt)-doped TiO₂ nanophotocatalysts: a smart approach for sustainable degradation of Rhodamine B dye, *Appl. Catal., B*, 181 (2016) 270–278.
- [66] K.M. Lee, S.B.A. Hamid, C.W. Lai, Multivariate analysis of photocatalytic-mineralization of Eriochrome Black T dye using ZnO catalyst and UV irradiation, *Mater. Sci. Semicond. Process.*, 39 (2015) 40–48.
- [67] D. Ollis, A. Mills, K. Lawrie, Kinetics of methylene blue (MB) photocatalyzed reduction and dark regeneration in a colorimetric oxygen sensor, *Appl. Catal., B*, 184 (2016) 201–207.
- [68] A. Duta, M. Visa, Simultaneous removal of two industrial dyes by adsorption and photocatalysis on a fly-ash-TiO₂ composite, *J. Photochem. Photobiol., A*, 306 (2015) 21–30.
- [69] G.G. Bessegato, J.C. Cardoso, M.V.B. Zanoni, Enhanced photoelectrocatalytic degradation of an acid dye with boron-doped TiO₂ nanotube anodes, *Catal. Today*, 240 (2015) 100–106.
- [70] Y.S. Karnikar, R.M. Dinde, N.M. Dinde, K.N. Bawankar, S.P. Hinge, A.V. Mohod, P.R. Gogate, Degradation of magenta dye using different approaches based on ultrasonic and ultraviolet irradiations: comparison of effectiveness and effect of additives for intensification, *Ultrason. Sonochem.*, 27 (2015) 117–124.
- [71] H.B. Hadjitaief, M.B. Zina, M.E. Galvez, P. Da Costa, Photocatalytic degradation of methyl green dye in aqueous solution over natural clay-supported ZnO-TiO₂ catalysts, *J. Photochem. Photobiol., A*, 315 (2016) 25–33.
- [72] M. Karatas, Y.A. Argun, M.E. Argun, Decolorization of anthraquinonic dye, Reactive Blue 114 from synthetic wastewater by Fenton process: kinetics and thermodynamics, *J. Ind. Eng. Chem.*, 18 (2012) 1058–1062.